

Central Lancashire Online Knowledge (CLOK)

Title	Shoreline change assessment in rapidly urbanizing coastal megacities using geospatial techniques
Type	Article
URL	https://clock.uclan.ac.uk/id/eprint/56779/
DOI	https://doi.org/10.3934/geosci.2025031
Date	2025
Citation	Kantamaneni, Komali, Li, Qiong, Makumbura, Randika K, Wu, Haotian, Zhu, Mingyu, Apostolopoulou, Athanasia, Xu, Weijie, Kenawy, Inji, Rajendran, Lakshmi Priya et al (2025) Shoreline change assessment in rapidly urbanizing coastal megacities using geospatial techniques. AIMS Geosciences, 11 (3). pp. 725-752.
Creators	Kantamaneni, Komali, Li, Qiong, Makumbura, Randika K, Wu, Haotian, Zhu, Mingyu, Apostolopoulou, Athanasia, Xu, Weijie, Kenawy, Inji, Rajendran, Lakshmi Priya, Jimenez-Bescos, Carlos, Ravichandran, Venkatesh, Pillai, Surendran Udayar and Rathnayake, Upaka

It is advisable to refer to the publisher's version if you intend to cite from the work.
<https://doi.org/10.3934/geosci.2025031>

For information about Research at UCLan please go to <http://www.uclan.ac.uk/research/>

All outputs in CLOK are protected by Intellectual Property Rights law, including Copyright law. Copyright, IPR and Moral Rights for the works on this site are retained by the individual authors and/or other copyright owners. Terms and conditions for use of this material are defined in the <http://clock.uclan.ac.uk/policies/>

Research article

Shoreline change assessment in rapidly urbanizing coastal megacities using geospatial techniques

Komali Kantamaneni^{1,2,*}, Qiong Li³, Randika K Makumbura⁴, Haotian Wu³, Mingyu Zhu⁵, Athanasia Apostolopoulou⁶, Weijie Xu⁷, Inji Kenawy⁸, Lakshmi Priya Rajendran⁹, Carlos Jimenez-Bescos¹⁰, Venkatesh Ravichandran¹¹, Surendran Udayar Pillai¹², and Upaka Rathnayake¹³

¹ School of Engineering, University of Central Lancashire, Preston PR1 2HE, United Kingdom

² United Nations- UK Regional Support Office, University of Central Lancashire, United Kingdom

³ School of Architecture, South China University of Technology, Wushan, Tianhe, Guangzhou 510640, China

⁴ Water Resources Management and Soft Computing Research Laboratory, Athurugiriya, 10150, Sri Lanka

⁵ School of Social & Political Sciences, University of Glasgow, United Kingdom

⁶ Nottingham Geospatial Institute, Nottingham University, 30 Triumph Rd, Lenton, Nottingham NG7 2TU, United Kingdom

⁷ Department of Architecture and Built Environment, University of Nottingham, University Park, Nottingham NG7 2RD, United Kingdom

⁸ School of Computing, Engineering and the Built Environment, Edinburgh Napier University, Merchiston Campus, 10 Colinton Road, Edinburgh EH10 5DT, United Kingdom

⁹ The Bartlett School of Architecture, The Bartlett Faculty of the Built Environment, University College London, Gower Street, London WC1E 6BT, United Kingdom

¹⁰ School of Built and Natural Environment, University of Derby, Kedleston Road, Derby DE22 1GB, United Kingdom

¹¹ Department of Civil Engineering, Indian Institutes of Technology–Guwahati, Assam, India

¹² ICAR- National Bureau of Soil Survey and Land Use Planning, Nagpur, India

¹³ Department of Civil & Construction, Faculty of Engineering and Design, Atlantic Technological University, Ash Lane, Sligo F91 YW50, Ireland

* **Correspondence:** Email: kkantamaneni@uclan.ac.uk.

Abstract: Coastal megacities face significant threats from various climate-induced hazards, including cyclones, storm surges, rising sea levels, coastal landslides, and floods. In recent decades, rapid urbanization and a range of anthropogenic pressures have exacerbated the vulnerability of these coastal regions. To assess the current level of coastal vulnerability, we focused on two Asian coastal megacities: Shenzhen and Shanghai. Using the Digital Shoreline Analysis System (DSAS) to evaluate coastal erosion vulnerability and shoreline changes from 1990 to 2022, we employed Shoreline Change Envelope (SCE) and Net Shoreline Movement (NSM) to measure the distance of shoreline change, while the rate of shoreline change was calculated with the End Point Rate (EPR). To simplify the DSAS analysis and highlight significant findings, Shenzhen's coastline was divided into two sections: The western coast (C1) and the eastern coastline (C2). The SCE results indicated a noteworthy seaward shoreline shift of 4.5 km in section C1 from 1990 to 2010, while section C2 experienced a significant alteration, extending 2.5 km seaward during the same period. In contrast, Shanghai exhibited a remarkable shoreline change, extending 6.5 km seaward between 1990 and 2010. NSM analysis revealed that within region C2, the maximum recorded erosion from 1990 to 2022 was 920 m, with the furthest observed accretion reaching 2,483 m. Additionally, results indicated that in section C1, the lowest shoreline change rate was -11.9 m/year, illustrating erosion, while Shanghai's minimum shoreline change rate was -3.04 m/year, also indicating a trend of erosion. The findings from this study, combined with the vulnerability maps, will aid policymakers and decision-makers in developing strategies to enhance the quality of life for coastal communities.

Keywords: coastal megacities; coastal erosion; China; shoreline changes; vulnerability assessment

1. Introduction

The cumulative impact of climate change and anthropogenic activities on coastal regions leads to an unstable coastal ecosystem, characterized by habitat loss and resource depletion, which is also vulnerable to various natural calamities, including floods, erosion, landslides, sea level rise, and pollution [1–3]. According to reports from the Intergovernmental Panel on Climate Change (IPCC), global warming has induced a significant threat to coastal communities and ecosystems due to rising sea levels. Furthermore, the global average temperature is increasing at a rate of 0.2 °C per decade [4–6]. Coastal megacities are the principal victims of the effects of climate change and rapid urbanization, which significantly impacts the coastal ecosystem and related factors [7]. Most economically significant megacities are in coastal environments, rendering them susceptible to the consequences of climate change, such as sea level rise, which is exacerbated by anthropogenic activities [8–10]. In comparison, the global sea level has risen in the 21st century, and it is predicted to accelerate by up to 65 ± 12 cm by the end of this century [11,12]. Coastal regions, recognized as vital ecological and socio-economic environments, exhibit significant vulnerability owing to the frequent occurrence of natural disasters [13]. According to Martínez et al. [14], coastal habitats contribute to 77% of the overall value of ecosystem services. Due to their transitory nature and the high volume of physical, biological, and

social interactions that occur, beaches confront a variety of environmental threats at local, regional, and global levels [14,15]. Numerous anthropogenic hazards, including emissions of pollutants, engineering alterations along coastal regions, overexploitation of coastal resources, and recreational activities, have adversely impacted coastal habitats.

Climate change significantly disrupts the environment, resulting in notable repercussions for human social and economic systems, especially in low-lying coastal regions. Due to their proximity to the ocean, coupled with high population density and substantial economic activity, coastal communities are more susceptible to the impacts of natural disasters compared to inland areas. Consequently, coastal regions are vulnerable to seawater intrusion, flooding attributable to storm surges, coastal erosion, water accumulation, and an increase in sea surface temperature [16]. Furthermore, coastal areas face heightened vulnerability to various environmental threats stemming from both natural and anthropogenic pressures and disturbances [17]. Coastal flooding, erosion, storms, and heat waves are prevalent events in the coastal cities of Asia, resulting from adverse climate change [18]. Similarly, the study by Hanson et al. [19] indicates that global coastal megacities are subject to significant consequences stemming from extreme climatic conditions, particularly in South Asian countries. The intensity and frequency of disasters, along with their associated economic losses within coastal regions of China, have been on an exponential rise [20,21]. Moreover, Zhang et al. [22] estimate that approximately 20% of coastal communities (around 350,000 individuals) are at high risk.

According to the Fifth Assessment Report published by the Intergovernmental Panel on Climate Change (IPCC), the risk to low-lying areas, particularly those adjacent to the coast, is anticipated to substantially increase throughout the 21st century and beyond [23]. Woodroffe [24] asserts that rising sea levels and increasing temperatures significantly affect the marine and coastal ecosystems of Asia. Liu et al. have conducted an analysis of coastal reclamation areas within the major Asian deltas since 1990, and their findings indicate that the implementation of coastal reclamation operations serves as the primary driver of modifications in coastline length and its shift towards the ocean [25]. Nearly 12% of Southeast Asian islands have experienced alterations in their coastal belt between 1990 and 2015, resulting in a loss of approximately 251 km² of land area [26]. Since 1988, about 22% of Australia's coastal zone has undergone significant modifications, with over 16% shifting at a rate exceeding 0.5 meters per year [27]. Between 1987 and 2017, the Transgressive Mahin Mud Coast of Nigeria experienced a 58% retreat (equivalent to 50.7 kilometers), culminating in a loss of 10.64 km² of land to the Atlantic Ocean [28]. Moreover, a 1.04-meter rise in sea level could threaten an area of 2,840.64 km² in Colombia under the worst-case scenario in the near future [29]. Additionally, a study by Chen J et al. predicts that certain coastal regions of China will experience a relative sea level rise of 5 to 8 mm per year. This increase could reach 30 to 45 centimeters by 2050 [30]. Approximately 68% of China's coastlines exhibit a tendency toward outward expansion, with an average weighted linear regression rate between the 1940s and 2014 of 24.30 meters per year [31]. Between 1979 and 2014, the total reclamation area along China's coast was approximately 11,162.89 km², with Shandong Province having the largest reclamation area at 2,736.54 km² [32].

Multifaceted coastal hazards, in conjunction with climate change, are increasing the vulnerability of coastal urban zones worldwide [33–35]. A significant portion of the world's coastlines are facing escalating environmental, physical, and socio-economic stresses, which present a major concern for stakeholders. Numerous coastal megacities and cities in China have developed and expanded due to rapid urbanization and the densely populated nature of coastal regions [36,37]. Conversely, ports,

which connect nations to the global economy through maritime trade, contribute to the improvement and development of specific countries and must not be overlooked [38]. While ports are essential for the fiscal development and prosperity of a country, they also contribute to environmental and ecological degradation that can adversely affect future communities. Coastal and shoreline alterations arise from various factors, including climate-induced hazards and anthropogenic pressures [39]. Seven of the world's largest ports are in China, with the Shenzhen port being one of them [40]. Numerous artificial structures play a vital role in protecting coastal areas, with jetties serving as a prime example. These critical structures facilitate safe navigation in and out of inlets [41]. However, jetties influence shoreline changes, sediment deposition, and wave propagation [42]. Coastal and shoreline transformations are key indicators of human-ecosystem interactions in these regions, and considerable changes have occurred over the past three decades [43].

Under these circumstances, assessments of coastal and climate vulnerability play a significant role in minimizing the effects of natural disasters. It is evident that the degree of sensitivity to climate change and exposure varies over time and location, specifically in terms of temporal and spatial factors. However, these assessments are also influenced by geography, population, economic conditions, societal factors, institutional frameworks, government policies, and the natural environment [44]. Consequently, evaluating vulnerability is essential for enhancing resilience and mitigating the risks posed by natural disasters to communities, societies, or nations. Coastal vulnerability evaluations can be categorized into two primary areas: The first type utilizes physical variables [45–48], while the second encompasses socio-economic variables, such as population density, economic damage, community perception, and others [49–52]. In the assessment and monitoring of coastal changes, particularly concerning physical coastal vulnerability, Remote Sensing (RS) and Geographic Information System (GIS) techniques play a vital role.

Identifying the vulnerability of coastal megacities, particularly in Asia, is of paramount importance due to the significant level of urbanization in the region. These vulnerability assessments will assist in generating new policies or revising existing ones to enhance the quality of life for individuals residing in coastal megacities. Accordingly, we emphasize a physical assessment utilizing physical variables, specifically coastal erosion and shoreline changes. Consequently, we aim to analyze the coastal zones of Shenzhen and Shanghai in China to provide a comprehensive understanding of coastal erosion and shoreline changes from 1990 to 2022. For numerous years, geospatial analysis has been a widely utilized technique for coastal vulnerability analysis, with several studies employing these methods [53–55]. As a result, we expect to capture the attention of the relevant authorities, enabling them to formulate a natural hazard mitigation plan and adequately prepare the community and population for both short- and long-term effects.

As highlighted in the preceding paragraphs, researchers have explored the impact of megacities, climate change, and shoreline alterations. However, this study is distinguished by its investigation into the assessment of coastal erosion and shoreline changes in two megacities, presenting a unique amalgamation of megacity and vulnerability concepts specific to China. It is imperative to conduct coastal assessments every three years, particularly in densely populated urban regions. We rigorously evaluated the vulnerability of coastal megacities, concentrating on coastal erosion and shoreline changes observed from 1910 to 2022.

As highlighted in the preceding paragraphs, numerous studies have examined the impacts of megacities, climate change, and shoreline alterations independently. However, there remains a

significant research gap in integrated assessments that simultaneously address shoreline dynamics and urban vulnerability within the context of rapidly developing megacities. We address this gap by uniquely combining the concepts of megacity growth and coastal vulnerability, focusing on two major Chinese coastal megacities viz., Shanghai and Shenzhen. By analyzing shoreline changes and coastal erosion from 1990 to 2022, this study offers a long-term perspective seldom covered in existing literature. Moreover, it highlights the need to conduct triennial coastal assessments in densely populated urban areas to support adaptive planning and risk mitigation strategies.

2. Study area—physical geography

The coastal region of China extends from the north to the south and is distinguished by diverse terrains and climatic conditions. The landscape within the northern coastal zone mostly consists of low hills and plains, with Hangzhou Bay serving as the defining boundary [56]. In comparison, the southern coastal area features low hills and plateaus, interspersed with numerous islands and intermittent estuarine delta plains [57,58]. In the coastal area of East Asia, the monsoons result in hot and humid summers, accompanied by cold and damp winters, with the highest temperatures occurring during the rainy season. Although the seasons do not adhere to a consistent pattern, the winters in the north are notably more severe than those in the south, while the summers in the south exhibit moderate temperatures. There is a discernible upward trend in both the annual mean temperature and the quantity of precipitation as one moves from the north to the south of China's coastal zone [59,60]. These spatial characteristics of the coastal region have culminated in the classification of its ecosystems into various categories. These categories include terrestrial ecosystems, shallow-water ecosystems, terrestrial-aquatic ecosystems, and marine-to-terrestrial transition ecosystems. These ecosystems play a vital role in providing a multitude of services that support and enhance human production and development. Such services encompass resource provision, natural process regulation, ecological function support, and the delivery of cultural benefits [61,62]. China's extensive coastline comprises municipalities, multiple provinces, and autonomous territories. These provinces and regions collectively house 42% of China's total population and contribute 60% of the nation's Gross Domestic Product (GDP) [62].

2.1. Case studies—coastal megacities

In this study, we focus on the Chinese Coastal Mega cities, specifically Shenzhen and Shanghai (see Figure 1), due to their geographical location and their physical and socioeconomic prospects. Shenzhen, positioned between 113 ° 45 ' 44 " E and 114 ° 37 ' 21 " E and 22 ° 26 ' 59 " N and 22 ° 51 ' 49 " N, encompasses an area of approximately 1, 996. 85 km² along the central coast of Guangdong Province. The city features a coastline of 260 kilometers, a population of 13 million, and an expansive marine area covering 1, 145 square kilometers [63]. The southern and central regions of Shenzhen are in proximity to Hong Kong. Given its placement in a tropical marine climate adjacent to South Asia, Shenzhen experiences all four seasons and receives significant precipitation throughout the year. Numerous extensive mudflats are observed along the relatively straight beach. This region is characterized by elevations ranging from 70 to 120 meters above mean sea level [64]. It is reasonable to infer that much of the shoreline along the eastern side of Shenzhen consists of bedrock, attributed to the dense vegetation and elevated terrain in this coastal segment. Conversely, the west coast of China

is predominantly straight with moderate elevations [65]. However, it is crucial to mention that a considerable portion of the western coastline comprises artificial structures, primarily resulting from Shenzhen's rapid urbanization and expansion. Shenzhen's GDP has grown at an average annualized rate exceeding 10% over the past two decades, marking it as one of the country's most dynamic regions and its first open city. The city hosts one of the world's most renowned ports, which has been bifurcated by the Kowloon Peninsula. Approximately 40 shipping companies maintain their headquarters at this port [66], consequently imposing several pressures on this coastal area. Situated in one of China's most vital coastal zones, Shenzhen serves as a crucial location for the realization of China's maritime ambitions and competitiveness in reform and development [67]. The rapid urbanization experienced by Shenzhen has prompted a significant inflow of the rural population into the urban center, further aggravating the scarcity of urban land [68]. Consequently, human activities have substantially altered the coastal landscape of Shenzhen.

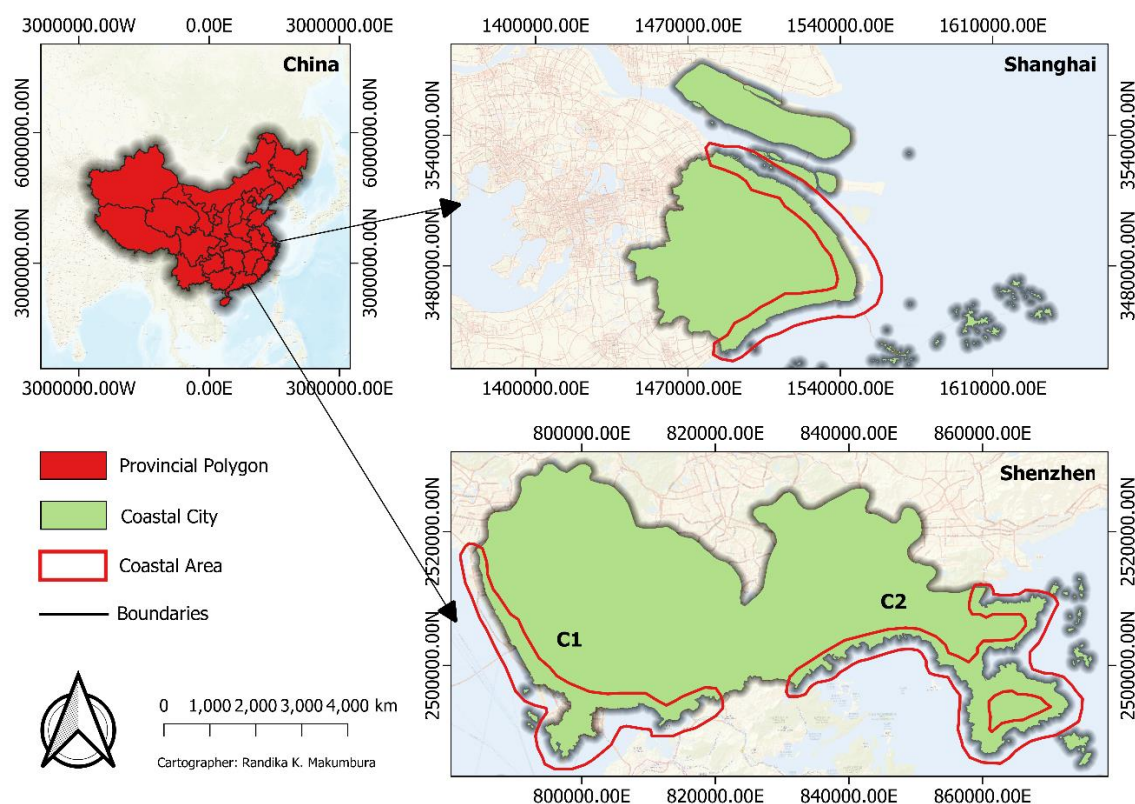


Figure 1. Location of the study area (top left; Shanghai, bottom left; Shenzhen).

Conversely, Shanghai is a low-lying and coastal modern megacity situated between $120^{\circ}51' E$ and $122^{\circ}12' E$, and $30^{\circ}40' N$ and $31^{\circ}53' N$. It is on both the eastern and western edges of Asia, encompassing approximately 6340 square kilometers of land and housing over 24 million residents [69]. The city possesses more than 300 square kilometers of urban land [70], with an additional 243 square kilometers developed between 2000 and 2004 as a result of rapid urbanization [71]. This city is also referred to as a megaport city and is recognized as one of the rapidly growing economies. Due to this rapid urbanization, Shanghai has experienced substantial construction of skyscrapers and significant

extraction of underground water. As the economic center of China, Shanghai is ranked among the wealthiest cities globally and is located in the Yangtze Estuary, an area sensitive to coastal changes driven by various factors, including fluctuations in sediment supply and sea level. Consequently, it is essential to monitor shoreline changes over time. Severe to extremely severe tropical cyclones frequently impact Shanghai, rendering this region more susceptible to coastal flooding [72]. Furthermore, Shanghai is a densely populated and economically advanced region; however, it remains one of the most highly exposed areas to the risks of compound flooding and coastal threats arising from heavy rainfall, erosion, and storm surges, attributable to its large population and high density of infrastructure (properties) [69]. As a result of climate change, urban expansion, the urban heat island effect, and rising relative sea levels, Shanghai faces multiple hazard risks and confronts various challenges such as cyclones, typhoons, storm surges, and extreme rainfall, even in the future [73].

3. Materials and methods

We assessed the vulnerability of coastal erosion and the changes in shorelines of two Chinese coastal megacities through the examination of various shoreline modifications. Shanghai and Shenzhen were selected as the focus of this study due to their unique and contrasting coastal dynamics, rapid urbanization patterns, contrasting coastal geomorphological settings, and strategic economic significance within China's eastern and southern seaboard. These cities represent two of the most prominent coastal megacities in China that have undergone extensive land reclamation, port development, and shoreline modifications over the past three decades [74–76]. While they do not represent all Chinese coastal regions, their selection provides valuable insights into the dynamics of coastal change in highly developed urban environments. The findings can offer a comparative framework for understanding similar trends in other rapidly developing coastal cities in China.

3.1. Analyzing coastal erosion and shoreline changes

Coastal erosion is a concern in nearly every coastal state. Both erosion and accretion have always existed, contributing to the formation of present-day coastlines. However, human activities have significantly exacerbated coastal erosion. We employed the Digital Shoreline Analysis System (DSAS), a widely adopted [77–79] tool developed by the United States Geological Survey (USGS) for shoreline change analysis, to examine the evolution of the coastlines of Shanghai and Shenzhen from 1990 to 2022, focusing on the years 1990, 2000, 2010, and 2022. The selection of the time span and frequency was based on initial investigations conducted through cloud computing techniques. To simplify matters, we chose a broad time span that captures the most significant changes in the study area. Intervals of at least 10 years were selected to effectively capture shoreline changes, given the 30m resolution of Landsat images. This longer time range is essential for visualizing changes, as shorelines need to be manually extracted. The DSAS add-on for ArcGIS offers a variety of statistical tools for analyzing data on coastline change, including the Shoreline Change Envelope (SCE), the Net Shoreline Movement (NSM), the End Point Rate (EPR), and the Linear Regression (LRR) [80]. As illustrated in Figure 1, we divided the Shenzhen coastline into two sections: The western coast (C1) and the eastern coastline (C2), to reduce the complexity of the DSAS analysis and provide noticeable findings from the study.

3.2. Data

The United States Geological Survey (USGS) Earth Explorer was employed to obtain Landsat images of the coastal megacities of Shanghai and Shenzhen. These Landsat images exhibited a spatial resolution of 30 by 30 meters and are accessible in raster format. The images were extracted utilizing Landsat 5 TM data from the years 1990, 2000, and 2010, as well as Landsat 8 OLI data from 2022 (refer to Table 1). The images were either cloudless or exhibited less than 10% cloud cover.

Table 1 Satellite data information, including sensors and bands.

Shenzhen					
Year	Satellite Name	Sensor ID	Path/Row	Acquisition Date	Band
1990	Landsat 5	TM	122/044	1990/10/13	Band 2
			121/044	1990/11/23	Band 4
2000	Landsat 5	TM	122/044	2000/01/02	Band 2
			121/044	2000/11/02	Band 4
2010	Landsat 5	TM	122/044	2010/09/18	Band 2
			121/044	2010/10/29	Band 4
2022	Landsat 9	OLI_TIRS	122/044	2022/12/24	Band 3
			121/044	2022/12/25	Band 5
Shanghai					
Year	Satellite Name	Sensor ID	Path/Row	Acquisition Date	Band
1990	Landsat 5	TM	118/038	1990/12/04	Band 2
			118/039		Band 4
2000	Landsat 5	TM	118/038	2000/06/06	Band 2
			118/039		Band 4
2010	Landsat 5	TM	118/038	2010/12/27	Band 2
			118/039		Band 4
2022	Landsat 9	OLI_TIRS	118/038	2022/12/20	Band 3
			118/039		Band 5

Shorelines were manually obtained utilizing the Normalized Difference Water Index (NDWI). Equation 1 delineates the calculation of the Normalized Difference Water Index (NDWI) based on the Near-Infrared (NIR) and Green (G) channels. To ensure reliability of manual shoreline digitization, accuracy checks were performed through cross-validation with high-resolution imagery (e.g., Sentinel-2, Google Earth Pro) for the corresponding years. Selected digitized shorelines were compared against identifiable coastal features such as seawalls, vegetation edges, or infrastructure in the high-resolution images.

$$NDWI = \frac{Green - Near\ Infrared\ (NIR)}{Green + Near\ Infrared\ (NIR)} \quad (1)$$

For Landsat 5;

$$NDWI = \frac{Band\ 2 - Band\ 4}{Band\ 2 + Band\ 4}$$

For Landsat 9;

$$NDWI = \frac{Band\ 3 - Band\ 5}{Band\ 3 + Band\ 5}$$

For this study, a threshold of 0.0 was applied to distinguish water ($NDWI > 0$) from land ($NDWI < 0$). This threshold was validated by overlaying NDWI-derived water masks onto high-resolution imagery to ensure accurate shoreline delineation.

4. Results and discussions

4.1. Coastal erosion

The Shoreline Change Envelope (SCE) and Net Shoreline Movement (NSM) methods offer insights into the shoreline's distance relative to each transect. However, it is important to understand that they do not directly convey the rate of shoreline change. SCE calculates the maximum distance between all shorelines without regard to the specific years linked to each coastline. Conversely, NSM measures the distance from the earliest shoreline (1990) to the most recent (2022). The End Point Rate (EPR) is then used to estimate the shoreline change rate by dividing the distance of the shoreline shift by the period between 1990 and 2022. Alternatively, the Long-Term Rate (LRR) requires fitting a least squares regression line to all shoreline points along a transect. Although LRR capitalizes on all available shorelines for a statistically sound analysis, it is also subject to the influence of outliers [81,82].

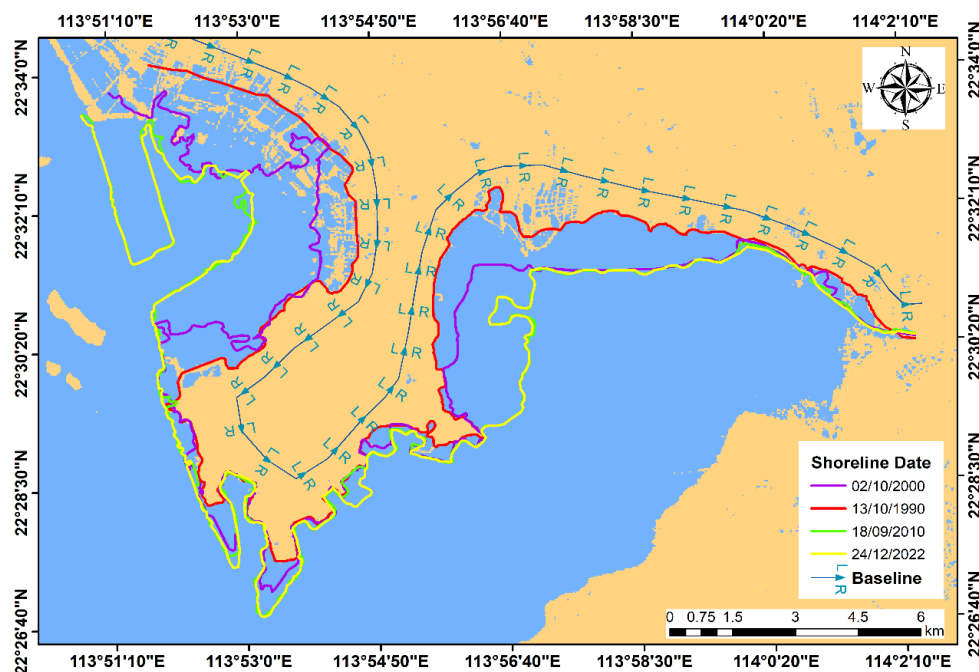
Thus, we employed the End Point Rate (EPR) method to evaluate the shoreline change rate. Positive values reflected accretion (shoreline advancement) for the NSM and EPR methods, while negative values signified erosion (shoreline retreat). In this research, a manually drawn baseline was fully positioned onshore, aligned with the other shorelines. These designated transects, starting from the baseline to each shoreline, formed the basis for statistical calculations. The points of intersection between these transects and the shorelines were analyzed to determine the distance and shoreline change rate in the coastal regions of Shanghai and Shenzhen.

4.1.1. Assessment of the shorelines in Shenzhen

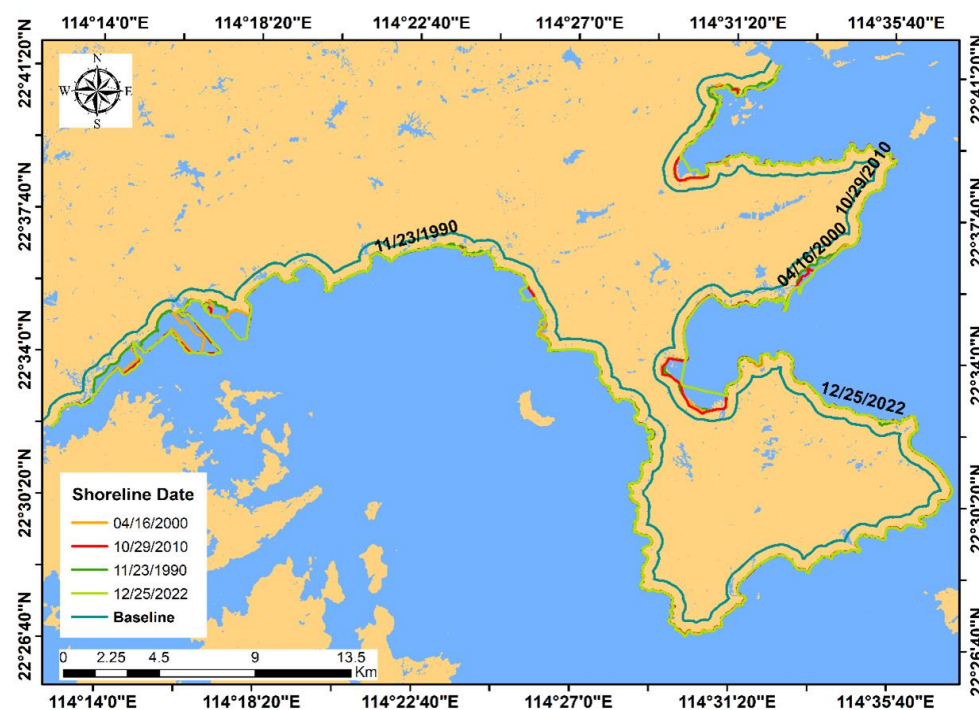
As demonstrated in Figure 2(a), the analysis of multi-temporal satellite imagery reveals a significant degree of dynamic shoreline change in the coastal zone of Shenzhen (C1). Similarly, Figure 2(b), which represents Shenzhen (C2), illustrates marked modifications in the locations of the shoreline over time, corresponding with the developments occurring near the shoreline.

SCE and NSM quantified the distance of shoreline change, whereas the rate of shoreline change was computed utilizing EPR. The findings of SCE in the C1 section (Figure 3) reveal that a significant alteration of the shoreline, measuring 4.5 km seaward, transpired between 1990 and 2010, indicative of accretion resulting from the extensively developed land use, which includes civil centers, a port,

and an expressway along the western coastlines. Consequently, following a considerable duration of rapid accretion and expansion from 1990 to 2010, the proportion of coastline undergoing accretion progressively diminished from 2010 to 2022. In contrast, the proportion of coastlines maintaining a stable state gradually increased, culminating in a relatively stable condition by 2022.



C1-(a)



C2- (b)

Figure 2. (a-b) Manually extracted Coastlines of Shenzhen (C1 (a) & C2 (b)) from 1990 to 2022 based on the Landsat images (1990, 2000, 2010, and 2022).

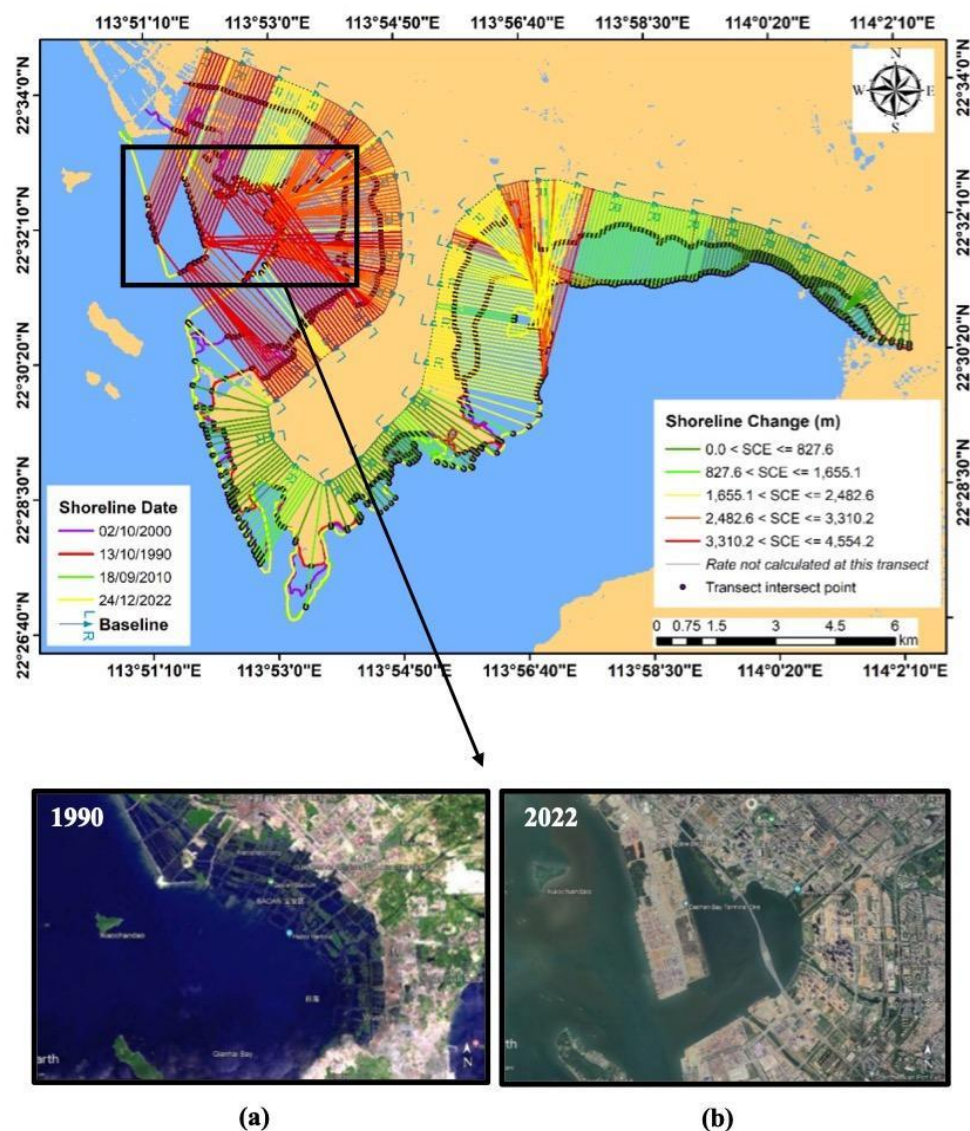


Figure 3. (a-b) Shoreline Change Envelope (SCE) from 1990 to 2022 based on DSAS results and illustration of the location where significant change has occurred from (a) 1990 to (b) 2022 in the Shenzhen coastline C1 section.

Correspondingly, the results of the Shoreline Change Evaluation (SCE) in the C2 section (Figure 4) indicate a significant modification of the shoreline, which has progressed 2.5 kilometers seaward from 1990 to 2010.

Figure 5(a) illustrates the distance between the shorelines in 1990 and 2022, as determined by the Net Shoreline Movement (NSM) method within the C1 section. The NSM analysis demonstrates that the most significant recorded erosion during the period from 1990 to 2022 was -381.2 m, while the greatest observed accretion was 4554.2 m. According to the NSM, the average extent of shoreline changes was calculated to be 1815 m. In comparison to the Shoreline Change Envelope (SCE) method, the NSM generates positive values (indicative of accretion) or negative values (indicative of erosion). Specifically, the NSM analysis reveals a positive value for the average shoreline change, suggesting that accretion, rather than erosion, is the predominant trend within the Shenzhen coastal region (C1).

In the coastal area of Shenzhen C2, as depicted in Figure 5(b), the NSM analysis indicates that the maximum recorded erosion from 1990 to 2022 was -920 m, and the furthest observed accretion was 2483 m. Furthermore, the NSM analysis highlights a positive average alteration in the shoreline, which indicates that accretion constitutes the prevailing trend in the Shenzhen coastal C2 region rather than erosion.

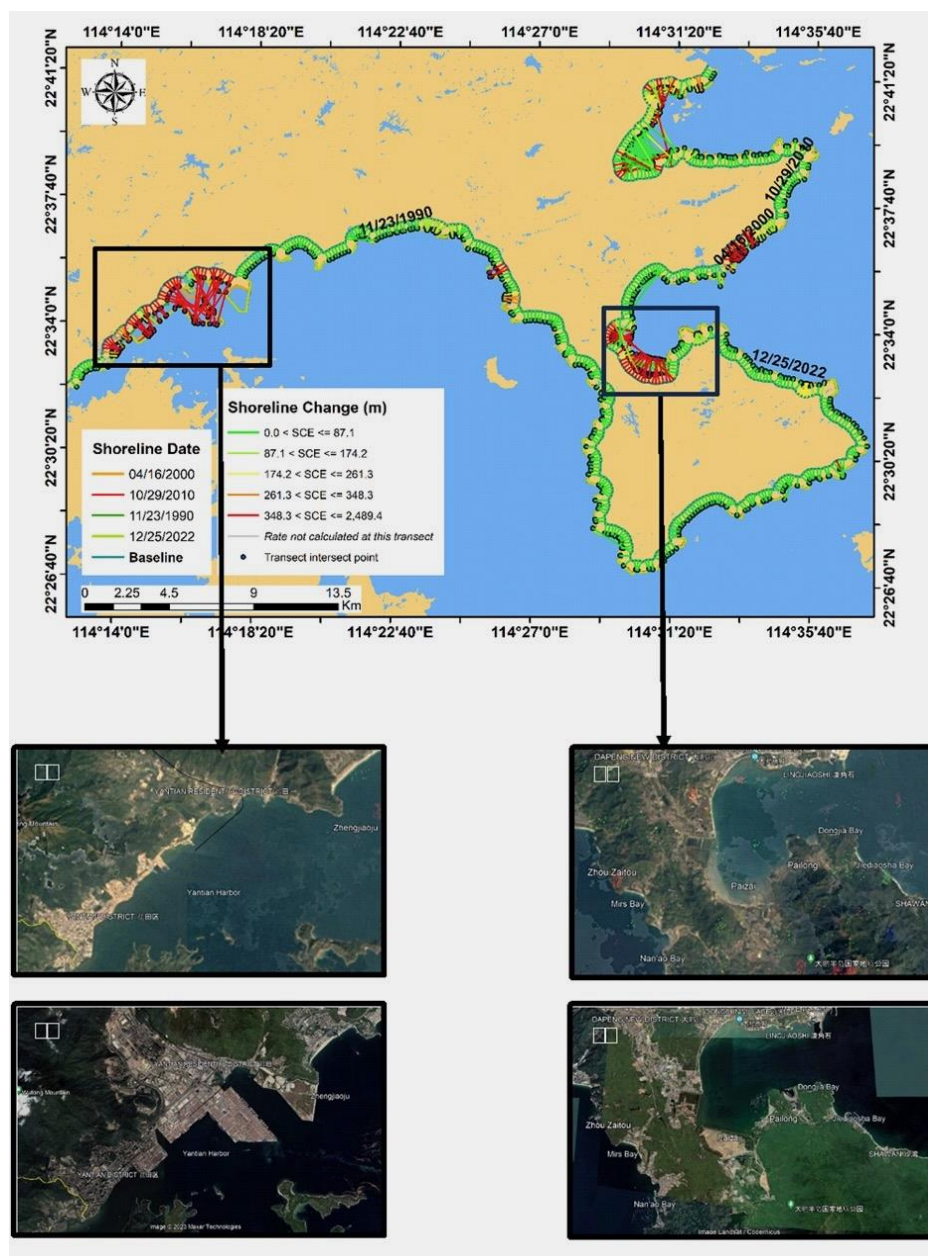
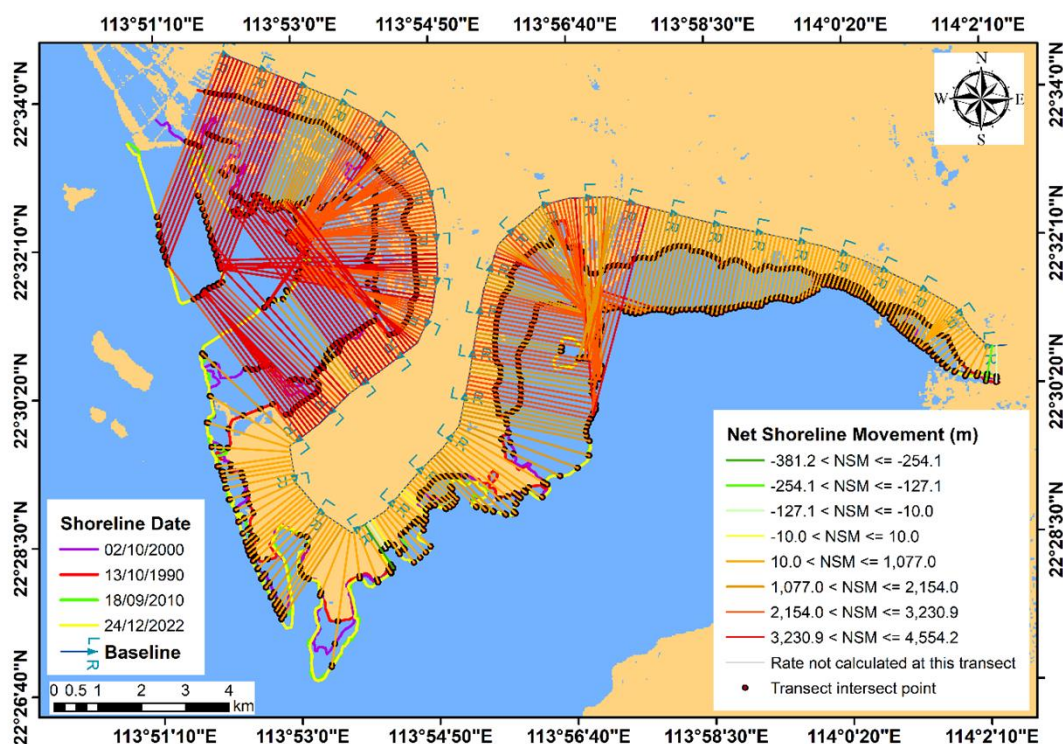
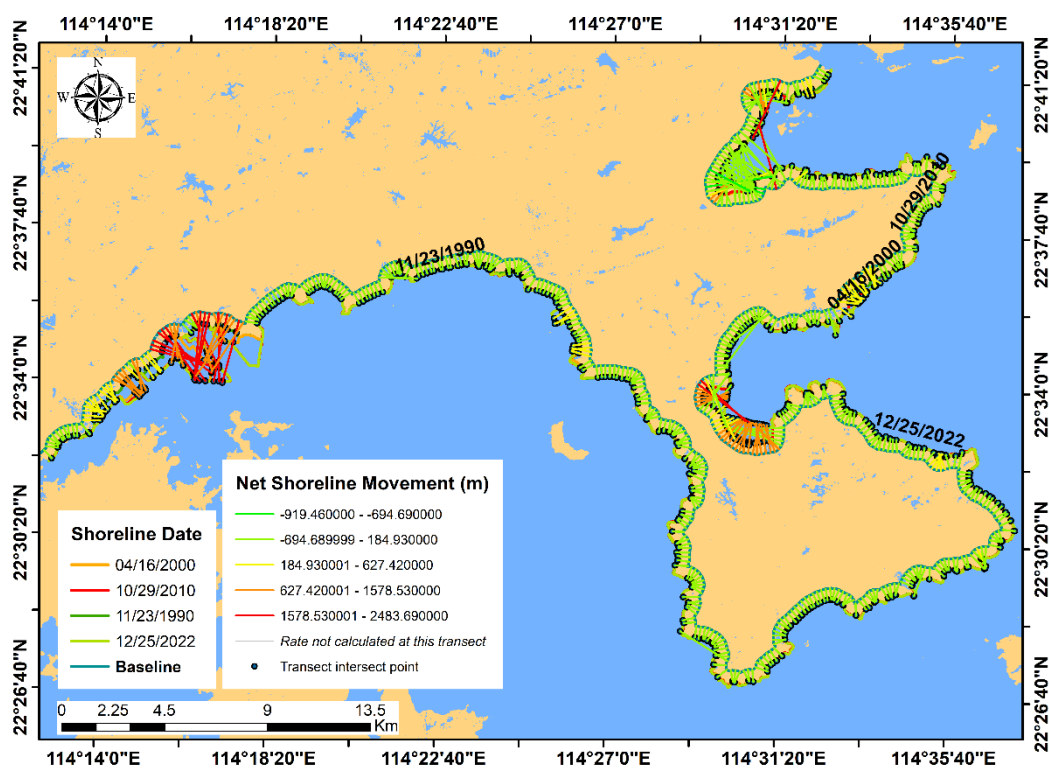


Figure 4. Shoreline Change Envelope (SCE) from 1990 to 2022 based on DSAS results and illustration of the location where significant change has occurred from 1990 to 2022 in the Shenzhen coastline C2 section.

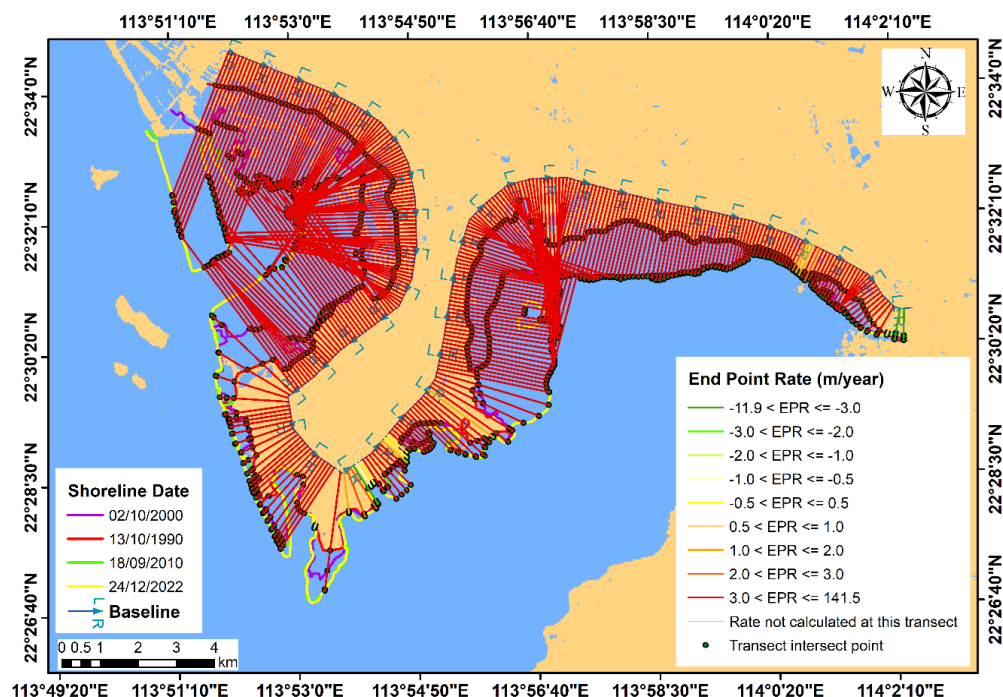


(a)

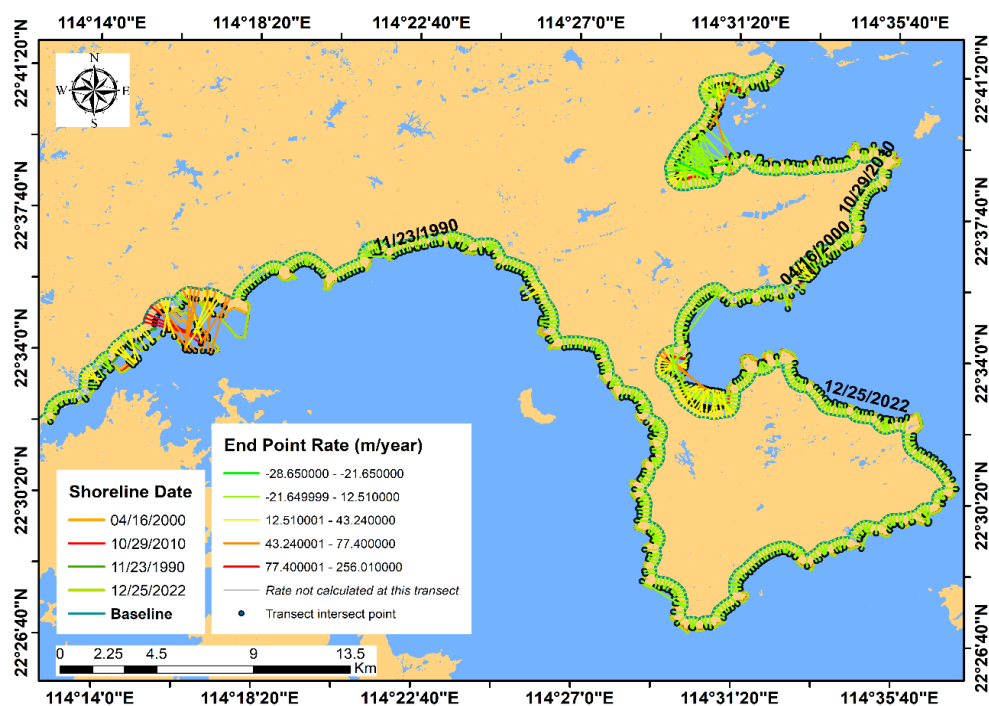


(b)

Figure 5. Net Shoreline Movement (NSM) from 1990 to 2022 based on DSAS results in the Shenzhen coastline (a) C1 & (b) C2 sections.



(a)



(b)

Figure 6. End Point Rate (EPR) from 1990 to 2022 based on DSAS results in the Shenzhen coastline (a) C1 & (b) C2 sections.

Figure 6(a) presents the rate of shoreline change, as determined by the End Point Rate (EPR) method, for the coastal region of Shenzhen (C1) between 1990 and 2022. Transect 163 exhibits the lowest shoreline change rate for the specified period, recorded at -11.9 m/year, indicating erosion due

to the negative rate. This observation is corroborated by the findings of NSM, which reported a maximum net shoreline movement of -381.2 m along the same transect. The average annual rate of shoreline change is positive, measuring 56.4 m. Likewise, Figure 6(b) indicates that the coastal region of Shenzhen (C2) experienced the lowest shoreline change rate of -28.65 m/year from 1990 to 2022, in conjunction with a maximum net shoreline movement of 256 meters. The average annual rate of shoreline change remains positive, amounting to 71.2 m.

The expansion of Shenzhen, particularly in the wake of China's reform and opening-up policies, underscores the city's notable advancements in both construction and economic sectors, alongside transformations in its coastline. As the inaugural special economic zone, the coastlines of Shenzhen have undergone significant changes due to human interventions. Research indicates that land reclamation and the establishment of embankments have been the predominant factors influencing these alterations, eclipsing the comparatively minor effects of natural phenomena such as tides and waves [54,63]. Moreover, Liu et al. (2017) [53] identified a robust correlation between changes in the coastline and socio-economic variables, indicating that population growth exerts a more substantial impact than economic metrics like GDP. This finding emphasizes the need to harmonize socio-economic development with population management to guarantee the sustainable development of coastal regions. The swift rise in population within coastal cities has not only catalyzed urban expansion but has also resulted in environmentally detrimental practices such as land reclamation.

4.2.1. Assessment of the Shorelines in Shanghai

Shanghai is recognized as one of the most highly developed cities in the world. Figure 7 illustrates a notable movement of the shoreline attributed to this development.

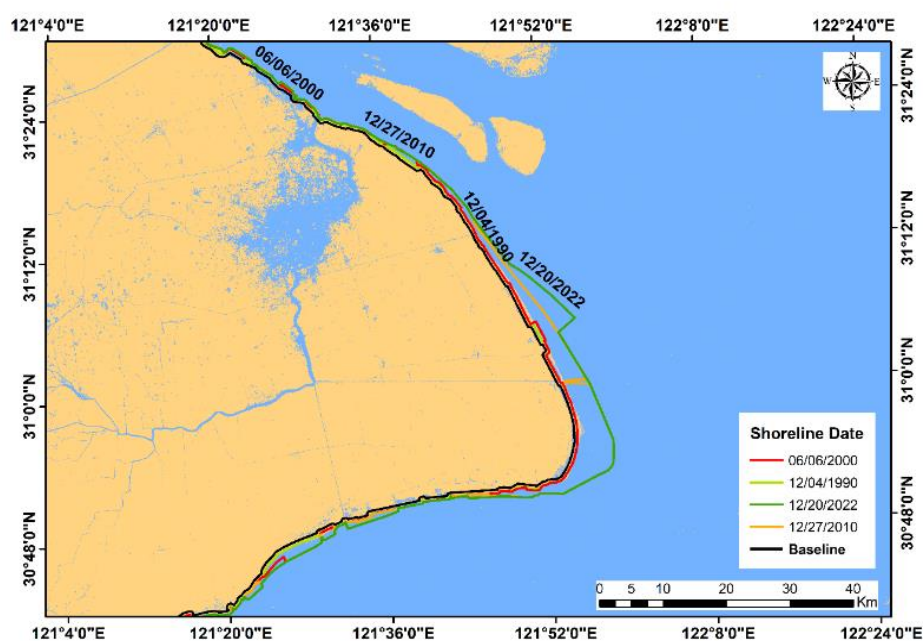


Figure 7. Manually extracted Coastlines of Shanghai from 1990 to 2022 based on the Landsat images (1990, 2000, 2010, and 2022).

Between 1990 and 2010, the shoreline did not undergo significant changes; however, considerable alterations transpired between 2010 and 2022 in Shanghai. These modifications are principally attributed to the substantial developments referenced earlier. Shoreline Change Evaluation (SCE) and Numerical Shoreline Modelling (NSM) methodologies were employed to evaluate the distance of shoreline change, whereas the rate of shoreline change was computed utilizing the Endpoint Rate (EPR) method. The results derived from the SCE analysis in Shanghai (Figure 8) indicate a substantial modification in the shoreline, extending 6.5 kilometers seaward from 1990 to 2010.

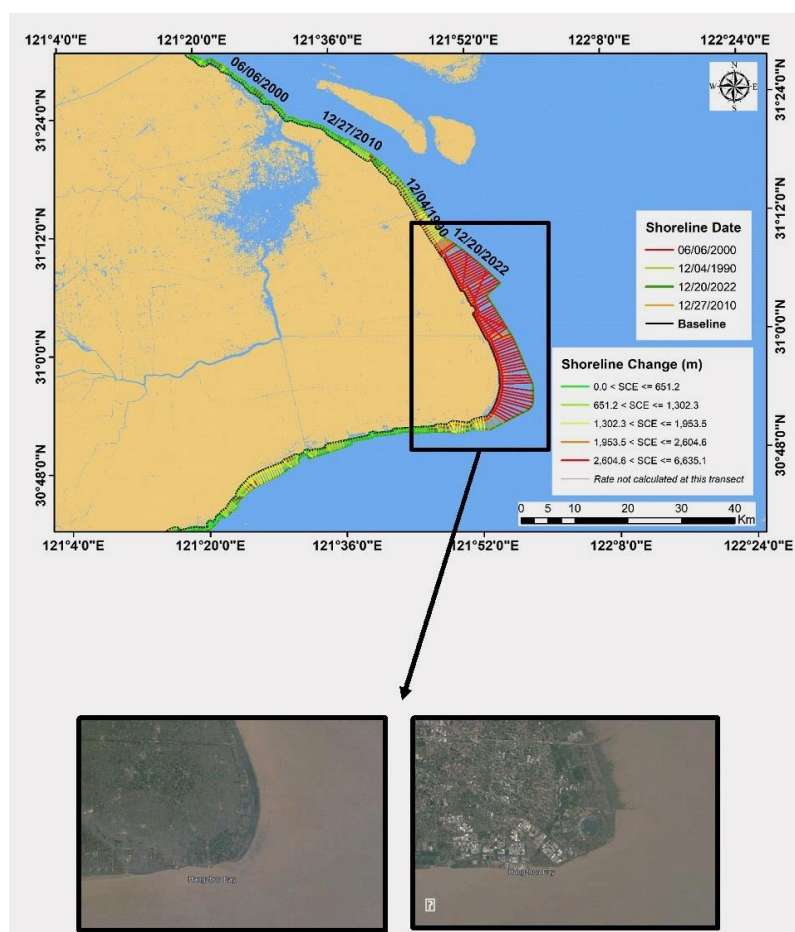


Figure 8. Shoreline Change Envelope (SCE) from 1990 to 2022 based on DSAS results and illustration of the location where significant change has occurred from (a) 1990 to (b) 2022 in Shanghai.

In Shanghai, as assessed by the Net Shoreline Movement (NSM) method, Figure 9 delineates the distance between shorelines in 1990 and 2022. During the period from 1990 to 2022, the NSM analysis demonstrates the absence of significant erosion, while the maximum observed accretion reaches 6635 m. Furthermore, the NSM analysis indicates a positive average shoreline change, implying that accretion, as opposed to erosion, is the predominant trend observed in the coastal region of Shanghai. Illustrated in Figure 10 is the rate of shoreline change, computed using the End Point Rate (EPR) method, in the coastal region of Shanghai for the years 1990 to 2022. The EPR method reveals the minimum shoreline change rate during 1990–2022, registering at -3.04 m/year, signifying a trend of erosion.

The alteration of Shanghai's shoreline has been significantly influenced by both natural conditions and anthropogenic activities. Positioned at the confluence of the Yangtze River and the Qiantang River, the sediment dynamics of the region assume a pivotal role in shaping the shoreline. Historical data obtained from the Datong gauging station on the Yangtze River indicate a remarkable decline in sediment discharge since the 1960s. This decline is predominantly attributed to extensive human activities, notably the operation of the Three Gorges Dam commencing in 2003 [64,65]. The dam has significantly modified the natural sediment load reaching the estuary, consequently leading to alterations in siltation and erosion patterns. In addition, the geomorphology of the Yangtze River estuary, distinguished by its intricate system of tidal channels and bifurcations, exerts influence over sediment transport and deposition. The estuary comprises four principal branches and several channels, including the North and South Branches, which are separated by Chongming Island. The South Branch further subdivides into the South Channel and North Channel, which are subsequently broken down into the North Passage and South Passage. These natural features determine the distribution and deposition of sediments along the shoreline, thereby contributing to its dynamic nature [66].

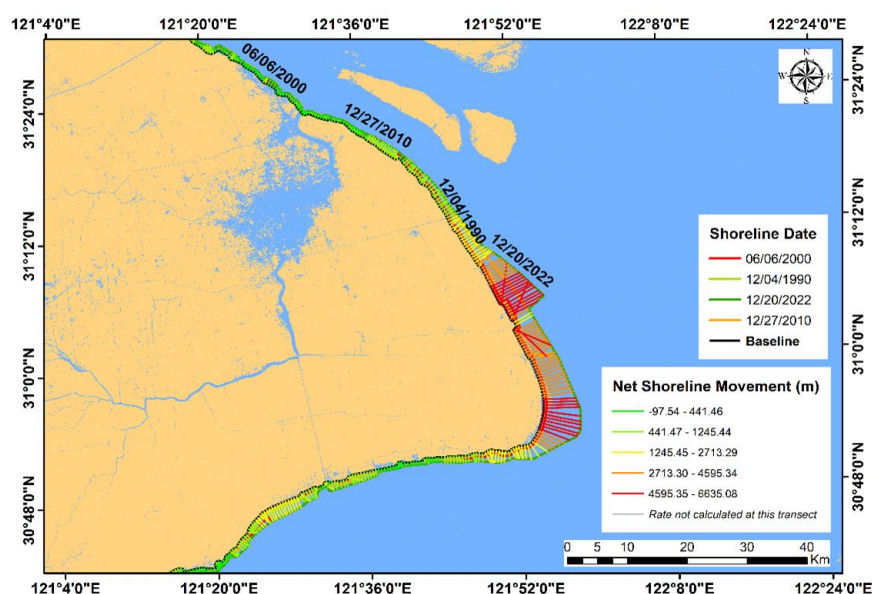


Figure 9. Net Shoreline Movement (NSM) from 1990 to 2022 based on DSAS results along the Shanghai coastline.

Anthropogenic modifications have significantly contributed to alterations in shoreline configurations. The rapid urbanization of Shanghai has necessitated extensive land reclamation initiatives to satisfy the demands of urban and socio-economic advancement. From 1949 to 2010, approximately 1040.9 km² of coastal wetlands in the Yangtze Estuary were reclaimed, as documented by the Shanghai Water Authority. This large-scale reclamation has expedited the transition of natural coastlines into urban areas, markedly transforming the shoreline. In addition to land reclamation, engineering projects related to waterways, which are essential for facilitating shipping- an integral element of Shanghai's economic progression, have affected tidal flows and sediment deposition patterns, thereby further influencing the evolution of the shoreline [67,68]. The cumulative impact of

diminished sediment supplies due to the Three Gorges Dam, alongside the extensive land reclamation and alterations to waterways, highlights the intricate interplay between natural processes and human interventions in the modification of Shanghai's shoreline. The overall summary of shoreline change statistics for Shenzhen and Shanghai coastal sections are given in Table 2.

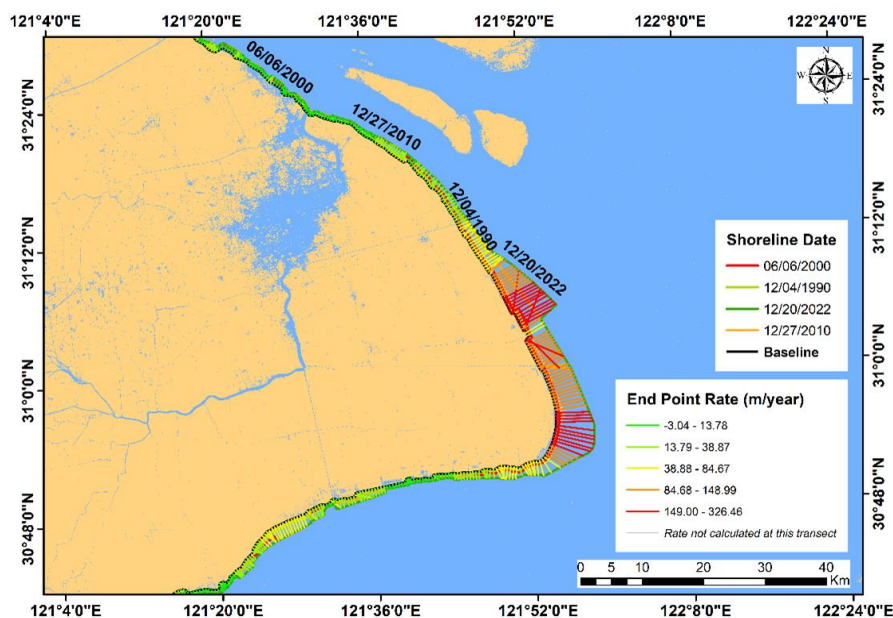


Figure 10. End Point Rate (EPR) from 1990 to 2022 based on DSAS results in Shanghai.

Table 2. Summary of Shoreline Change Statistics for Shenzhen and Shanghai Coastal Sections.

City	Section	Max Accretion (m)	Max Erosion (m)	Avg. Shoreline Movement (NSM, m)	Avg. Change Rate (EPR, m/year)
Shenzhen	C1	4554.2	381.2	1815	56.4
	C2	2483	920	1380	71.2
Shanghai	S1	6635	98	3250	3.04

4.2. Coastal urban megacities and trends

Coastal urban megacities in Asia have undergone rapid growth, surpassing their counterparts in Europe and America. According to UN-DESA [83,84], between 1975 and 2000, the number of megacities escalated from two to thirteen, particularly within low- and middle-income nations. Of the twenty-three global megacities, sixteen are along coastlines [85]. The swift expansion of these cities across the globe, especially in China, has resulted in an increase in climate-induced hazards such as sea level rise, typhoons, flooding, landslides, and the urban heat island effect, thereby posing a significant threat to communities [86]. During disasters, urban slums exhibit greater vulnerability compared to affluent communities, as evidenced by the 2005 flooding in Mumbai, which disproportionately affected slum residents and the urban poor [83,84].

Coastal megacities present both opportunities and incentives for economic and social growth in contemporary China [86]. However, the assessment of coastal risks in urban megacities is not comprehensive, attributed to various factors, including the complex interactions among environmental, social, and anthropogenic dynamics. Our findings indicate that two Chinese coastal urban megacities, Shenzhen and Shanghai, both of which maintain world-class ports, continue to experience coastal vulnerabilities resulting from an array of natural and anthropogenic hazards. This research illuminated the susceptibility of these two megacities by analyzing coastal and shoreline alterations from 1990 to 2022. Notably, both study areas demonstrate substantial changes to their coastlines and shorelines. Although port structures are generally deemed effective in mitigating coastal erosion rates [33], this phenomenon was not evident in the instances of Shenzhen and Shanghai. The extensive land reclamation in Shanghai between 1990 and 2015, coupled with the over-exploitation and atypical utilization of coastal regions, particularly the conversion of wetland areas into constructed environments, has posed significant threats to ecological security [87,88]. Consequently, land reclamation should be curtailed in critical zones, including Shanghai. The rate of human-induced urban construction, expansion, and redevelopment in Shenzhen is similarly high, akin to that in Shanghai [89]. This study suggests that coastal accretion represents the predominant trend within the coastal area of Shenzhen, particularly in the second phase (C2). The results of this research indicate that shoreline changes in both regions are substantial and may negatively impact communities and infrastructure if prompt action is not taken.

4.2.1. Coastal Management Strategies

The rapid urban expansion observed along the coastlines of Shanghai and Shenzhen has presented opportunities and significant challenges for sustainable coastal management. These cities, while economically vibrant, are increasingly exposed to coastal hazards due to their geographic positioning, anthropogenic pressures, and the impacts of climate change. Shanghai has long relied on extensive engineered defenses, including concrete seawalls, revetments, and reclaimed land platforms, especially in the Pudong and Chongming areas. These hard structures have offered protection against storm surges but have also disrupted natural sediment transport and estuarine dynamics. In contrast, Shenzhen, with its relatively more recent coastal development, has adopted a combination of engineered barriers and soft measures in select zones, such as mangrove rehabilitation projects in the Shenzhen Bay area. However, both cities exhibit limited integration of adaptive management strategies that consider long-term sea-level rise and hydrodynamic feedbacks.

4.2.2. Coastal typology

To better understand how coastal dynamics vary spatially, we mapped the coastal types across both cities, distinguishing areas as urbanized coastlines, which are dominant in central Shanghai and western Shenzhen and often reclaimed and highly altered with impervious surfaces. Besides, natural bedrock coasts is limited in extent, observed in the southern Shenzhen region, and relatively stable but constrained in developmental capacity. With respect to unconsolidated coasts, it is observed along the Yangtze Delta margins in Shanghai and the eastern fringes of Shenzhen; highly dynamic and vulnerable to erosion and flooding. This typological mapping helps contextualize the observed variability in shoreline change rates. Urbanized and unconsolidated zones show the highest rates of

shoreline advancement and retreat respectively, suggesting that engineered interventions and sediment instability jointly influence coastal behavior.

4.2.3. Elevation and vulnerability

Elevation data reveal that large portions of both cities' coastal belts lie below 5 meters above mean sea level, with certain reclaimed zones in Shanghai even lying at or below high tide levels. This low elevation, when coupled with dense urban settlement, makes these areas extremely vulnerable to storm surges, extreme rainfall events, and projected sea-level rise. However, current coastal planning documents rarely account for elevation-based risk zoning, which is critical for long-term resilience.

Similar to our findings, other major coastal megacities such as Mumbai, Manila, and Lagos have experienced significant shoreline modifications driven by rapid urbanization, extensive land reclamation, and altered sediment dynamics [90–93]. For example, studies in Mumbai report substantial accretion and erosion linked to coastal infrastructure projects and monsoonal influences, while Manila's shoreline dynamics reflect the combined effects of typhoon impacts and urban expansion. Lagos, on the other hand, exhibits notable shoreline erosion primarily due to rising sea levels and reduced sediment supply. These comparisons highlight that, despite regional differences, megacities worldwide face common challenges of balancing coastal development with natural coastal processes, emphasizing the broader relevance of our findings.

5. Limitations and future research

This study presents several limitations. One notable limitation is the exclusion of critical socio-economic, cultural, and political variables that are essential for a more comprehensive assessment of coastal vulnerability. While these data were omitted primarily due to accessibility challenges and inconsistencies in publicly available datasets, it is important to acknowledge that other researchers, such as those employing Integrated Coastal Vulnerability Index (ICVI) or Social Vulnerability Index (SVI) frameworks, have successfully incorporated socio-economic dimensions (e.g., population density, income level, infrastructure exposure, governance quality) to evaluate vulnerability with a more holistic lens [94–96]. Researchers should build upon such frameworks to enhance the comprehensiveness of vulnerability assessments in coastal megacities.

Furthermore, the availability of continuous, open-access data concerning certain physical parameters, such as mean significant wave height, complex engineering structures, and high-resolution areal maps, is limited. Consequently, we were unable to evaluate physical vulnerability comprehensively. Moreover, physical oceanographic processes generally play a crucial role in coastal changes, independent of anthropogenic activities. The physical processes influencing these amplitudes include the convergence and divergence of tidal and wave energy, which can lead to erosion or accretion. Although tectonic activity primarily governs the broader features of the coastline, rivers significantly contribute to sediment supply to the shore, thereby aiding in the maintenance of erosional and accretionary trends. In the future, we aim to expand by incorporating socio-economic and additional physical parameters. Moreover, a comprehensive assessment of more Asian coastal megacities will be conducted to establish a ranking of vulnerable cities.

Last, this study is subject to uncertainties associated with estimating shoreline positions using

medium-resolution satellite imagery, such as Landsat (30 m spatial resolution). Errors may arise from various sources, including pixel resolution, georeferencing inaccuracies, the tidal stage at the time of image acquisition, and the subjectivity involved in digitization. Future research could mitigate these uncertainties by integrating higher-resolution satellite imagery (e.g., Sentinel-2, commercial platforms) alongside automated shoreline extraction techniques.

6. Recommendations

The following are recommendations based on current research to enhance the conditions in the designated case study areas:

1. Establishing nature-based solutions such as dunes and mangroves.
2. Developing cost-effective coastal protection measures, comprising both soft and hard engineering structures or filter units.
3. Enacting regulations and enforcing a strict prohibition on new constructions and redevelopment activities in proximity to the shoreline.
4. Controlling unauthorized human settlements in these two coastal megacities.
5. Investing in operational research aimed at mitigating coastal erosion and improving shoreline management.
6. Ensuring unrestricted access to open data, which includes nighttime data.
7. Managing seawater intrusions.
8. Conducting regular monitoring of underground storm and flood regulations, as well as floodwater storage facilities in both cities.
9. Generating rigorous public awareness regarding coastal erosion and shoreline changes.

7. Conclusions

The impact of climate change on coastal vulnerability constitutes a significant concern for global infrastructure, communities, urban areas, and megacities, particularly in developing Asian countries such as China. Thus, it is imperative to continuously monitor and assess changes in coastlines and shorelines to formulate effective management strategies in China's coastal regions. This study has demonstrated that physical variables and processes substantially influence the alteration of shorelines and the occurrence of coastal erosion. Moreover, spatial tools, such as the Digital Shoreline Analysis System (DSAS), were employed to calculate changes over various temporal scales. Our findings indicated considerable seaward shifts along the western coast of Shenzhen and an extension along the eastern coast from 1990 to 2010, attributable to extensive developmental activities. Both natural and anthropogenic alterations have significantly contributed to changes in coastal and shoreline configurations. The Net Shoreline Movement (NSM) analysis revealed erosion and accretion patterns along the western and eastern coasts. The average annual rate of shoreline change was positive, with the lowest rate recorded at -28.65 meters per year and the highest at 256 meters. In Shanghai, the rate of shoreline change was -3.04 meters per year from 1990 to 2022, indicating a prevailing erosion trend in the region. The alterations in Shanghai's shoreline have been markedly influenced by natural conditions and human activities. This comprehensive study of two coastal megacities in China provides critical insights into dynamic shoreline changes and coastal erosion, which are essential for developing

effective mitigation strategies against natural hazards. Continuous monitoring of satellite data is crucial for predicting future shoreline changes and minimizing potential damages. The study advocates for the development of integrated Coastal Zone Management plans aimed at improving conditions in both cities to effectively address future challenges and constraints.

Author contributions

KK and RKM wrote the initial manuscript, performed the analysis; QL, HW, MZ, AA, WX, IK, LPR, CJB, VR, and SUP worked on the manuscript; UR supervised the work, revised and reviewed the manuscript.

Use of AI tools declaration

The authors declare they have not used Artificial Intelligence (AI) tools in the creation of this article.

Funding

This research was funded by British Council -Challenge Prize.

Data availability

Certain level of data will be available based upon the request.

Conflict of interest

The authors declare no conflict of interest.

References

1. Hoegh-Guldberg O, Bruno JF (2010) The impact of climate change on the world's marine ecosystems. *Science* 328: 1523–1528. <https://doi.org/10.1126/science.1189930>
2. Duarte C, Losada I, Hendriks I, et al. (2013) The role of coastal plant communities for climate change mitigation and adaptation. *Nature Clim Change* 3: 961–968. <https://doi.org/10.1038/nclimate1970>
3. Huang F, Xu Y, Tan Z, et al. (2018) Assessment of pollutions and identification of sources of heavy metals in sediments from west coast of Shenzhen, China. *Environm Sci Pollut Res* 25: 3647–3656. <https://doi.org/10.1007/s11356-017-0362-y>
4. IPCC, Climate change 2007—the physical science basis, 2007. Available from: https://www.ipcc.ch/site/assets/uploads/2020/02/ar4-wg1-sum_vol_en.pdf.
5. Rosenzweig C, Karoly D, Vicarelli M, et al. (2008) Attributing physical and biological impacts to anthropogenic climate change. *Nature* 453: 353–357. <https://doi.org/10.1038/nature06937>
6. Wood R (2008) Natural ups and downs. *Nature* 453: 43–45. <https://doi.org/10.1038/453043a>

7. Murali RM, Riyas MJ, Reshma KN, et al. (2020) Climate change impact and vulnerability assessment of Mumbai city, India. *Nat Hazards* 102: 575–589. <https://doi.org/10.1007/s11069-019-03766-2>
8. Nicholls RJ (1995) Coastal megacities and climate change. *GeoJournal* 37: 369–379. <https://doi.org/10.1007/BF00814018>
9. Young AF (2013) Coastal megacities, environmental hazards and global environmental change, *Megacities and the Coast*, Routledge, 70–99.
10. Griggs G, Reguero BG (2021) Coastal adaptation to climate change and sea-level rise. *Water* 13: 2151. <https://doi.org/10.3390/w13162151>
11. Kopp RE, Kemp AC, Bittermann K, et al. (2016) Temperature-driven global sea-level variability in the Common Era. *PNAS* 113: E1434–E1441. <https://doi.org/10.1073/pnas.1517056113>
12. Nerem RS, Beckley BD, Fasullo JT, et al. (2018) Climate-change-driven accelerated sea-level rise detected in the altimeter era. *PNAS* 115: 2022–2025. <https://doi.org/10.1073/pnas.1717312115>
13. Eggert H, Olsson B (2009) Valuing multi-attribute marine water quality. *Mar Policy* 33: 201–206. <https://doi.org/10.1016/j.marpol.2008.05.011>
14. Martínez ML, Intralawan A, Vázquez G, et al. (2007) The coasts of our world: Ecological, economic and social importance. *Ecol Econ* 63: 254–272. <https://doi.org/10.1016/j.ecolecon.2006.10.022>
15. de Andrade MMN, Szlafsztein CF, Souza-Filho PWM, et al. (2010) A socioeconomic and natural vulnerability index for oil spills in an Amazonian harbor: A case study using GIS and remote sensing. *J Environ Manage* 91: 1972–1980. <https://doi.org/10.1016/j.jenvman.2010.04.016>
16. Torresan S, Critto A, Dalla Valle M, et al. (2008) Assessing coastal vulnerability to climate change: comparing segmentation at global and regional scales. *Sustain Sci* 3: 45–65. <https://doi.org/10.1007/s11625-008-0045-1>
17. Kantamaneni K, Phillips M, Thomas T, et al. (2018) Assessing coastal vulnerability: Development of a combined physical and economic index. *Ocean Coast Manage* 158: 164–175. <https://doi.org/10.1016/j.ocecoaman.2018.03.039>
18. Kantamaneni K, Li Q, Wu H, et al. (2023) Towards a Combined Physical and Social Evaluation of Climate Vulnerability in Coastal Urban Megacities. *Water* 15: 712. <https://doi.org/10.3390/w15040712>
19. Hanson S, Nicholls R, Ranger N, et al. (2011) A global ranking of port cities with high exposure to climate extremes. *Climatic Change* 104: 89–111. <https://doi.org/10.1007/s10584-010-9977-4>
20. Yin J, Yin Z, Wang J, et al. (2012) National assessment of coastal vulnerability to sea-level rise for the Chinese coast. *J Coast Conserv* 16: 123–133. <https://doi.org/10.1007/s11852-012-0180-9>
21. Qin W, Lin A, Fang J, et al. (2017) Spatial and temporal evolution of community resilience to natural hazards in the coastal areas of China. *Nat Hazards* 89: 331–349. <https://doi.org/10.1007/s11069-017-2967-3>
22. Zhang Y, Wu T, Arkema KK, et al. (2021) Coastal vulnerability to climate change in China's Bohai Economic Rim. *Environ Int* 147: 106359. <https://doi.org/10.1016/j.envint.2020.106359>
23. Pachauri RK, Allen MR, Barros VR, et al. (2014) *Climate change 2014: synthesis report. Contribution of Working Groups I, II and III to the fifth assessment report of the Intergovernmental Panel on Climate Change*, Ipcc.

24. Woodroffe CD (2010) Assessing the vulnerability of Asian megadeltas to climate change using GIS, *Coastal and Marine Geospatial Technologies. Coastal Systems and Continental Margins*, Springer, Dordrecht. https://doi.org/10.1007/978-1-4020-9720-1_36, 379–391.
25. Liu Y, Li J, Sun C, et al. (2023) Thirty-year changes of the coastlines, wetlands, and ecosystem services in the Asia major deltas. *J Environ Manage* 326: 116675. <https://doi.org/10.1016/j.jenvman.2022.116675>
26. Zhang Y, Li D, Fan C, et al. (2021) Southeast Asia island coastline changes and driving forces from 1990 to 2015. *Ocean Coast Manage* 215: 105967. <https://doi.org/10.1016/j.ocecoaman.2021.105967>
27. Bishop-Taylor R, Nanson R, Sagar S, et al. (2021) Mapping Australia’s dynamic coastline at mean sea level using three decades of Landsat imagery. *Remote Sens Environ* 267: 112734. <https://doi.org/10.1016/j.rse.2021.112734>
28. Dada OA, Agbaje AO, Adesina RB, et al. (2019) Effect of coastal land use change on coastline dynamics along the Nigerian Transgressive Mahin mud coast. *Ocean Coast Manage* 168: 251–264. <https://doi.org/10.1016/j.ocecoaman.2018.11.014>
29. Nevermann H, Becerra Gomez JN, Fröhle P, et al. (2023) Land loss implications of sea level rise along the coastline of Colombia under different climate change scenarios. *Clim Risk Manag* 39: 100470. <https://doi.org/10.1016/j.crm.2022.100470>
30. Chen J (1997) The impact of sea level rise on China’s coastal areas and its disaster hazard evaluation. *J Coastal Res* 1997: 925–930.
31. Hou X, Wu T, Hou W, et al. (2016) Characteristics of coastline changes in mainland China since the early 1940s. *Sci China Earth Sci* 59: 1791–1802. <https://doi.org/10.1007/s11430-016-5317-5>
32. Meng W, Hu B, He M, et al. (2017) Temporal-spatial variations and driving factors analysis of coastal reclamation in China. *Estuarine Coastal Shelf Sci* 191: 39–49. <https://doi.org/10.1016/j.ecss.2017.04.008>
33. Kantamaneni K, Gallagher A, Du X (2019) Assessing and mapping regional coastal vulnerability for port environments and coastal cities. *J Coast Conserv* 23: 59–70. <https://doi.org/10.1007/s11852-018-0636-7>
34. Moser SC, Jeffress Williams S, Boesch DF (2012) Wicked challenges at land’s End: Managing coastal vulnerability under climate change. *Ann Rev Env Resour* 37: 51–78. <https://doi.org/10.1146/annurev-environ-021611-135158>
35. Laino E, Iglesias G (2023) Extreme climate change hazards and impacts on European coastal cities: A review. *Renewable Sustainable Energy Rev* 184: 113587. <https://doi.org/10.1016/j.rser.2023.113587>
36. Pelling M, Blackburn S (2012) Megacities and the Coast: Risk, Resilience, and Transformation. 2013: Earthscan from Routledge. Available from: <https://www.book2look.com/embed/9781135074746>
37. Su S, Pi J, Wan C, et al. (2015) Categorizing social vulnerability patterns in Chinese coastal cities. *Ocean Coast Manage* 116: 1–8. <https://doi.org/10.1016/j.ocecoaman.2015.06.026>
38. Saengsupavanich C, Chitsom L, Sanitwong-Na-Ayutthaya S, et al. (2023) Land-based physical and biological environmental mitigation measures of a mega port construction in Thailand. *E3S Web of Conferences*, 422: 03002. <https://doi.org/10.1051/e3sconf/202342203002>

39. Newton A, Icely J, Cristina S, et al. (2020) Anthropogenic, direct pressures on coastal wetlands. *Front Ecol Evol* 8: 144. <https://doi.org/10.3389/fevo.2020.00144>
40. Wang H, Mao X, Rutherford D (2015) Costs and benefits of shore power at the port of Shenzhen. *The International Council on Clean Transportation (ICCT)*.
41. Saengsupavanich C, Yun LS, Lee LH, et al. (2022) Intertidal intercepted sediment at jetties along the Gulf of Thailand. *Front Mar Sci* 9: 970592. <https://doi.org/10.3389/fmars.2022.970592>
42. Ghashemizadeh N, Tajziehchi M (2013) Impact of Long Jetty on Shoreline Evaluation (Case Study: Eastern Coast of Bandar Abbas). *J Basic Appl Sci Res* 2090–4304.
43. Tian H, Xu K, Goes JI, et al. (2020) Shoreline changes along the coast of mainland China—time to pause and reflect? *ISPRS Int J Geo-Inf* 9: 572. <https://doi.org/10.3390/ijgi9100572>
44. Field CB, Barros V, Stocker TR, et al. (2012) Managing the risks of extreme events and disasters to advance climate change adaptation: special report of the intergovernmental panel on climate change. Cambridge University Press. Available from: <https://www.ipcc.ch/report/managing-the-risks-of-extreme-events-and-disasters-to-advance-climate-change-adaptation/>.
45. Gornitz V (1990) Vulnerability of the East Coast, USA to future sea level rise. *J Coastal Res*, 201–237.
46. Gornitz VM, Daniels RC, White TW, et al. (1997) The development of a coastal risk assessment database: vulnerability to sea-level rise in the US Southeast. *J Coastal Res*, 327–338.
47. Shaw J, Taylor RB, Forbes DL, et al. (1998) *Sensitivity of the coasts of Canada to sea-level rise*, Geological Survey of Canada Ottawa. <https://doi.org/10.4095/210075>
48. Thieler ER, Hammar-Klose ES (2000) National assessment of coastal vulnerability to sea-level rise: preliminary results for the US Gulf of Mexico Coast. US Geological survey. Available from: <https://pubs.usgs.gov/dds/dds68/reports/gulfrep.pdf>.
49. Boruff BJ, Emrich C, Cutter SL (2005) Erosion hazard vulnerability of US coastal counties. *J Coastal Res* 21: 932–942. <https://doi.org/10.2112/04-0172.1>
50. Murali RM (2013) Interactive comment on “Coastal vulnerability assessment of Puducherry coast, India using analytical hierarchical process” by R. Mani Murali et al. *Nat Hazards Earth Syst Sci Discuss* 1: C684–C687.
51. Kunte PD, Jauhari N, Mehrotra U, et al. (2014) Multi-hazards coastal vulnerability assessment of Goa, India, using geospatial techniques. *Ocean Coast Manage* 95: 264–281. <https://doi.org/10.1016/j.ocecoaman.2014.04.024>
52. Mahapatra M, Ramakrishnan R, Rajawat AS (2015) Coastal vulnerability assessment using analytical hierarchical process for South Gujarat coast, India. *Nat Hazards* 76: 139–159. <https://doi.org/10.1007/s11069-014-1491-y>
53. Mahendra R, Mohanty PC, Bisoyi H, et al. (2011) Assessment and management of coastal multi-hazard vulnerability along the Cuddalore—Villupuram, east coast of India using geospatial techniques. *Ocean Coast Manage* 54: 302–311. <https://doi.org/10.1016/j.ocecoaman.2010.12.008>
54. Islam MA, Hossain MS, Murshed S (2015) Assessment of coastal vulnerability due to sea level change at Bhola Island, Bangladesh: using geospatial techniques. *J Indian Soc Remote Sens* 43: 625–637. <https://doi.org/10.1007/s12524-014-0426-0>
55. Hadipour V, Vafaie F, Kerle N (2020) An indicator-based approach to assess social vulnerability of coastal areas to sea-level rise and flooding: A case study of Bandar Abbas city, Iran. *Ocean Coast Manage* 188: 105077. <https://doi.org/10.1016/j.ocecoaman.2019.105077>

56. Wang X (2017) Variation of Extreme Climate and Its Impact on NDVI in the Coastal Area of China. *University of Chinese Academy of Sciences*. In Chinese.
57. Han Q, Huang X, Xing Q, et al. (2012) A review of environment problems in the coastal sea of South China. *Aquat Ecosyst Health Manage* 15: 108–117. <https://doi.org/10.1080/14634988.2012.687611>
58. Pedoja K, Shen JW, Kershaw S, et al. (2008) Coastal Quaternary morphologies on the northern coast of the South China Sea, China, and their implications for current tectonic models: A review and preliminary study. *Mar Geol* 255: 103–117. <https://doi.org/10.1016/j.margeo.2008.02.002>
59. Shi P, Sun S, Wang M, et al. (2014) Climate change regionalization in China (1961–2010). *Sci China Earth Sci* 57: 2676–2689. <https://doi.org/10.1007/s11430-014-4889-1>
60. Wang X, Li Y, Wang M, et al. (2021) Changes in daily extreme temperature and precipitation events in mainland China from 1960 to 2016 under global warming. *Int J Climatol* 41: 1465–1483.
61. Su K, Wei D, Lin W (2020) Evaluation of ecosystem services value and its implications for policy making in China—A case study of Fujian province. *Ecol Indic* 108: 105752. <https://doi.org/10.1016/j.ecolind.2019.105752>
62. Li K, Zhang L, Chen B, et al. (2023) Analysis of China's Coastline Changes during 1990–2020. *Remote Sens* 15: 981. <https://doi.org/10.3390/rs15040981>
63. Feng T, Xu N (2021) Satellite-based monitoring of annual coastal reclamation in Shenzhen and Hong Kong since the 21st Century: A comparative study. *J Mar Sci Eng* 9: 48. <https://doi.org/10.3390/jmse9010048>
64. Wu X, Liu C, Wu G (2018) Spatial-temporal analysis and stability investigation of coastline changes: A case study in Shenzhen, China. *IEEE J Sel Top Appl Earth Obs Remote Sens* 11: 45–56. <https://doi.org/10.1109/JSTARS.2017.2755444>
65. Liu C, Wu X, Cao X, et al. (2017) Analysis of coastline changes and the socio-economic driving mechanisms in Shenzhen, China. *Mar Geod* 40: 378–403. <https://doi.org/10.1080/01490419.2017.1319447>
66. Ship Hub the Port of Shenzhen, 2024. Available from: <https://www.porttechnology.org/news/top-5-ports-in-china-2024/>.
67. Yi G, Su F, Sun X, et al. (2011) A study on driving forces of land use change of Guangdong Province coastal zone and islands in recent 20 a. *Haiyang Xuebao* 33: 95–103.
68. Weng Q (2002) Land use change analysis in the Zhujiang Delta of China using satellite remote sensing, GIS and stochastic modelling. *J Environ Manage* 64: 273–284. <https://doi.org/10.1006/jema.2001.0509>
69. Xu H, Tian Z, Sun L, et al. (2022) Compound flood impact of water level and rainfall during tropical cyclone periods in a coastal city: the case of Shanghai. *Nat Hazards Earth Syst Sci* 22: 2347–2358. <https://doi.org/10.5194/nhess-22-2347-2022>
70. Zhao M, Cai H, Qiao Z, et al. (2016) Influence of urban expansion on the urban heat island effect in Shanghai. *Int J Geogr Inf Sci* 30: 2421–2441. <https://doi.org/10.1080/13658816.2016.1178389>
71. NASA Earth Observatory, 2024. Available from: <https://earthobservatory.nasa.gov/>.
72. Yin J, Lin N, Yang Y, et al. (2021) Hazard assessment for typhoon-induced coastal flooding and inundation in Shanghai, China. *JGR Oceans* 126: e2021JC017319. <https://doi.org/10.1029/2021JC017319>

73. Wang J, Yi S, Li M, et al. (2018) Effects of sea level rise, land subsidence, bathymetric change and typhoon tracks on storm flooding in the coastal areas of Shanghai. *Sci Total Environ* 621: 228–234. <https://doi.org/10.1016/j.scitotenv.2017.11.224>
74. Yeung H (2015) A tale of two cities—the development and reform experiences of Shenzhen and Shanghai. *J Chinese Econ Bus Stud* 13: 369–396. <https://doi.org/10.1080/14765284.2015.1090268>
75. Wei X, Li H, Yang N, et al. (2015) Changes in the perceived quality of primary care in Shanghai and Shenzhen, China: a difference-in-difference analysis. *Bull W H O* 93: 407–416.
76. Xiaobin ZS, Qionghua L, Ming CN (2013) The rise of China and the development of financial centres in Hong Kong, Beijing, Shanghai, and Shenzhen. *J Globalization Stud* 4: 32–62.
77. de Oliveira EB, Barboza EG (2023) A multi-scale assessment of shoreline changes at an undeveloped beach in southern Brazil. *J South Am Earth Sci* 131: 104632. <https://doi.org/10.1016/j.jsames.2023.104632>
78. de Oliveira EB, Barboza EG (2024) Shoreline change assessment at Arroio do Sal (Southern Brazil) using different shoreline extraction methods. *Remote Sens Appl Soc Environ* 36: 101303. <https://doi.org/10.1016/j.rsase.2024.101303>
79. Nassar K, Mahmod WE, Fath H, et al. (2019) Shoreline change detection using DSAS technique: Case of North Sinai coast, Egypt. *Mar Georesour Geotechnol* 37: 81–95. <https://doi.org/10.1080/1064119X.2018.1448912>
80. Thieler ER, Himmelstoss EA, Zichichi JL, et al. (2009) *The Digital Shoreline Analysis System (DSAS) version 4.0—an ArcGIS extension for calculating shoreline change*, US Geological Survey. <https://doi.org/10.3133/ofr20081278>
81. Dolan R, Fenster MS, Holme SJ (1991) Temporal analysis of shoreline recession and accretion. *J Coastal Res* 7: 723–744.
82. Brooks S, Spencer T (2010) Temporal and spatial variations in recession rates and sediment release from soft rock cliffs, Suffolk coast, UK. *Geomorphology* 124: 26–41. <https://doi.org/10.1016/j.geomorph.2010.08.005>
83. Heilig GK (2012) World urbanization prospects: the 2011 revision. United Nations, Department of Economic and Social Affairs (DESA). *Population Division*, New York, 14: 555.
84. Blackburn S, Pelling M, Marques C (2019) Megacities and the coast: global context and scope for transformation. *Coasts Estuaries*, 661–669. <https://doi.org/10.1016/B978-0-12-814003-1.00038-1>
85. Coastal megacities: risks and opportunities, 2014. Available from: <http://www.igbp.net/news/features/features/coastalmegacitiesrisksandopportunities.5.62dc35801456272b46d17b.html>.
86. Tang P, Zhong W, Wen J, et al. (2023) Developing and understanding cascading effects scenario of typhoons in coastal mega-cities from system perspectives for disaster risk reduction: A case study of shenzhen, China. *Int J Disaster Risk Reduct* 92: 103691. <https://doi.org/10.1016/j.ijdr.2023.103691>
87. Zhang Y, Chen R, Wang Y (2020) Tendency of land reclamation in coastal areas of Shanghai from 1998 to 2015. *Land Use Policy* 91: 104370. <https://doi.org/10.1016/j.landusepol.2019.104370>
88. Liu Y, Li J, Yang Y (2018) Strategic adjustment of land use policy under the economic transformation. *Land Use Policy* 74: 5–14. <https://doi.org/10.1016/j.landusepol.2017.07.005>

89. Xia C, Zhai G (2023) Territorial spatial vulnerability assessment based on PSO-BP neural network: A case study in Shenzhen, China. *Ecol Inf* 75: 102088. <https://doi.org/10.1016/j.ecoinf.2023.102088>
90. Pelling M, Blackburn S (2014) Case studies: Governing social and environmental transformation in coastal megacities, *Megacities and the Coast*, Routledge, 200–236.
91. Mega VP (2016) *Conscious coastal cities*, Springer Cham, New York, USA. <https://doi.org/10.1007/978-3-319-20218-1>
92. Li H (2003) Management of coastal mega-cities—a new challenge in the 21st century. *Mar Policy* 27: 333–337. [https://doi.org/10.1016/S0308-597X\(03\)00045-9](https://doi.org/10.1016/S0308-597X(03)00045-9)
93. Bruns A (2014) The environmental impacts of megacities on the coast, *Megacities and the Coast*, Routledge, 22–69.
94. Theocharidis C, Prodromou M, Doukanari M, et al. (2025) Integrated Coastal Vulnerability Index (ICVI) Assessment of Protaras Coast in Cyprus: Balancing Tourism and Coastal Risks. *Geographies* 5: 12. <https://doi.org/10.3390/geographies5010012>
95. Charuka B, Angnuureng DB, Brempong EK, et al. (2023) Assessment of the integrated coastal vulnerability index of Ghana toward future coastal infrastructure investment plans. *Ocean Coast Manage* 244: 106804. <https://doi.org/10.1016/j.ocecoaman.2023.106804>
96. Tano RA, Aman A, Toualy E, et al. (2018) Development of an integrated coastal vulnerability index for the Ivorian coast in West Africa. *J Environ Prot* 9: 1171. <https://doi.org/10.4236/jep.2018.911073>



AIMS Press

© 2025 the Author(s), licensee AIMS Press. This is an open access article distributed under the terms of the Creative Commons Attribution License (<https://creativecommons.org/licenses/by/4.0>)